

Versatility in the Coordination Modes of *n*-Chlorobenzoato Ligands: Synthesis, Structure and Magnetic Properties of Three Types of Polynuclear Mn^{II} Compounds

Verónica Gómez^{*[a]} and Montserrat Corbella^[a]

Keywords: Manganese / Carboxylate ligands / Coordination modes / Magnetic properties / EPR spectroscopy

Three different types of polynuclear manganese(II) compounds with chlorobenzoato bridges were obtained from the reaction of $\text{Mn}(n\text{-ClC}_6\text{H}_4\text{COO})_2$ with 1,10-phenanthroline (phen): three trinuclear compounds $[\text{Mn}_3(\mu\text{-}n\text{-ClC}_6\text{H}_4\text{COO})_6(\text{phen})_2]$ with $n = 2, 3, 4$ (**1–3**), one one-dimensional system $[\text{Mn}(\mu\text{-}3\text{-ClC}_6\text{H}_4\text{COO})_2(\text{phen})]_n$ (**4**) and one neutral dinuclear compound $[\{\text{Mn}(4\text{-ClC}_6\text{H}_4\text{COO})(\text{phen})\}_2(\mu\text{-}4\text{-ClC}_6\text{H}_4\text{COO})_2(\mu\text{-H}_2\text{O})]$ (**5**). Compounds **1**, **3**, **4** and **5** were characterized by X-ray diffraction and show four different coordination modes for the carboxylate ligand: as a bidentate bridge in a *syn-syn* mode or *syn-anti* mode, as a monodentate bridge and as a terminal monodentate ligand. The five compounds show weak antiferromagnetic coupling; the *J* values are -2.9 , -2.8 ,

-2.8 , -1.8 and -3.6 cm^{-1} for compounds **1–5**, respectively. Each type of compound may be distinguished by their characteristic EPR spectrum at 4 K. Fairly good simulations of the spectra at 4 K for the trinuclear compounds **1–3** were obtained with ground state ZFS parameters, $D_{5/2}$ and $E_{5/2}$, of 0.16 cm^{-1} and 0.05 cm^{-1} (**1**), 0.16 cm^{-1} and 0.043 cm^{-1} (**2**) and 0.16 cm^{-1} and 0.053 cm^{-1} (**3**), respectively. For the dinuclear complex **5**, the best simulation of the spectrum at 4 K was obtained with ZFS parameters of the ion, D_{Mn} and E_{Mn} , of 0.187 cm^{-1} and 0.061 cm^{-1} , respectively.

(© Wiley-VCH Verlag GmbH & Co. KGaA, 69451 Weinheim, Germany, 2009)

Introduction

Polynuclear manganese compounds with carboxylate ligands are of great interest in bioinorganic chemistry^[1] and molecular magnetism.^[2] In the former, several compounds have been synthesized to mimic the active sites of various metalloproteins, such as catalase^[3] and the oxygen-evolving complex (OEC) of photosystem II.^[4] In the latter, it was discovered that some compounds characterized by a large-spin ground state and an appreciable magnetoanisotropy could behave as single-molecule magnets (SMMs) at very low temperatures.^[5]

Manganese complexes containing carboxylate ligands have been extensively studied. Carboxylate groups display a wide variety of coordination modes such as monodentate terminal, chelating, bidentate bridging and monodentate bridging modes (Figure 1), which lead to several types of compounds. There are some trinuclear compounds with a $[\text{Mn}_3(\mu\text{-RCOO})_6]$ core reported in the literature,^[6–23] but only half of them are magnetically studied,^[13–22] and even less have been characterized by EPR spectroscopy.^[19–23] The number of described 1D Mn^{II} chains with two carbox-

ylate bridges is few;^[21–22,24–33] not many of them are magnetically characterized,^[21,22,24] and there are even fewer studied by EPR spectroscopy.^[21,22] With regard to dinuclear Mn^{II} compounds, there are not many compounds with a $[\text{Mn}_2(\mu\text{-H}_2\text{O})(\mu\text{-RCOO})_2]^{2+}$ core reported in the literature,^[34–44] and fewer whose magnetic properties have been studied^[41–44] or whose EPR spectrum have been reported.^[44]

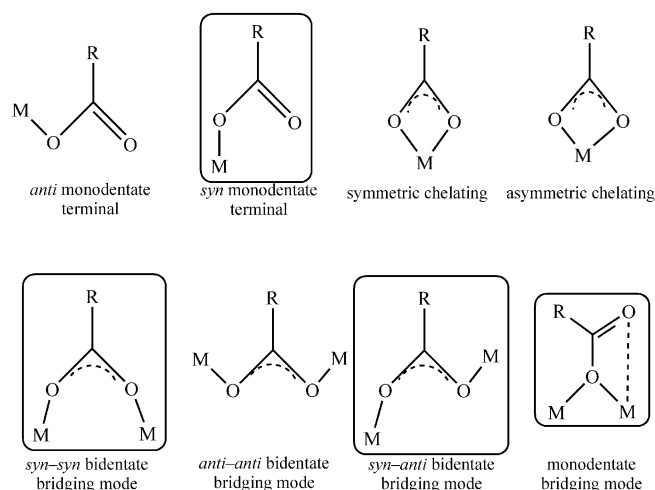


Figure 1. Carboxylate binding modes in metal complexes. Bridges involved in the compounds reported here are framed.

[a] Departament de Química Inorgànica, Universitat de Barcelona, Martí i Franquès 1–11, 08028 Barcelona, Spain
Fax: +34-934907725

E-mail: veronica.gomez@qi.ub.es

Supporting information for this article is available on the WWW under <http://dx.doi.org/10.1002/ejic.200900532>.

Here, we report the synthesis and characterization of three types of Mn^{II} compounds with different nuclearity, with chlorobenzoato and 1,10-phenanthroline ligands: three trinuclear compounds $[\text{Mn}_3(\mu\text{-}n\text{-ClC}_6\text{H}_4\text{COO})_6(\text{phen})_2]$, where $n = 2, 3, 4$ (**1**–**3**), one 1D compound $[\text{Mn}(\mu\text{-}3\text{-ClC}_6\text{H}_4\text{COO})_2(\text{phen})]_n$ (**4**) and one neutral dinuclear compound $[\{\text{Mn}(4\text{-ClC}_6\text{H}_4\text{COO})(\text{phen})\}_2(\mu\text{-}4\text{-ClC}_6\text{H}_4\text{COO})_2(\mu\text{-H}_2\text{O})]$ (**5**). Structural characterization of compounds **1**, **3**–**5** was achieved by X-ray diffraction. The magnetic behaviour and EPR spectra of all compounds were studied.

Results and Discussion

Previously,^[21] we reported the reaction between $[\text{Mn}(n\text{-ClC}_6\text{H}_4\text{COO})_2] \cdot n\text{H}_2\text{O}$ ($n = 2, 3, 4$) and 2,2'-bipyridine in ethanol, using two different Mn^{II} /bpy ratios (3:2 or 1:1) to obtain two different neutral compounds: trinuclear complexes and 1D systems. In the present work, we carried out the analogous reaction with 1,10-phenanthroline instead of bpy, and used two different solvents, ethanol and acetonitrile. In this case, depending on the molar ratio and/or solvent, three types of compounds were obtained.

With 2- $\text{ClC}_6\text{H}_4\text{COO}$, only the trinuclear complex $[\text{Mn}_3(\mu\text{-}2\text{-ClC}_6\text{H}_4\text{COO})_6(\text{phen})_2]$ (**1**) was obtained, regardless of the Mn^{II} /phen ratio or solvent ($\text{CH}_3\text{CH}_2\text{OH}$ or CH_3CN), as reported for the reaction with bpy.^[21]

With 3- $\text{ClC}_6\text{H}_4\text{COO}$, two compounds were obtained in both solvents: the trinuclear compound $[\text{Mn}_3(\mu\text{-}3\text{-ClC}_6\text{H}_4\text{COO})_6(\text{phen})_2]$ (**2**) when the Mn^{II} /phen ratio was 3:2 and the 1D system $[\text{Mn}(\mu\text{-}3\text{-ClC}_6\text{H}_4\text{COO})_2(\text{phen})]_n$ (**4**) when the ratio was 1:1. This behaviour is different from that reported for the analogous reactions with bpy,^[21] where, for both Mn^{II} /bpy ratios, the trinuclear compound was obtained and the 1D system appeared as a by-product after filtration of the trinuclear complex.

With 4- $\text{ClC}_6\text{H}_4\text{COO}$, independent of the Mn^{II} /phen ratio, the trinuclear compound $[\text{Mn}_3(\mu\text{-}4\text{-ClC}_6\text{H}_4\text{COO})_6(\text{phen})_2]$ (**3**) was obtained using ethanol as solvent. The analogous reactions with bpy lead to the formation of a 1D compound.^[21] Using acetonitrile as solvent, with both Mn^{II} /phen ratios, the neutral dinuclear compound $[\{\text{Mn}(4\text{-ClC}_6\text{H}_4\text{COO})(\text{phen})\}_2(\mu\text{-}4\text{-ClC}_6\text{H}_4\text{COO})_2(\mu\text{-H}_2\text{O})]$ (**5**) was obtained. This compound had been previously reported in the literature,^[38,39] but was obtained by different procedures and shows small structural differences.

Description of the Structures

$[\text{Mn}_3(\mu\text{-}n\text{-ClC}_6\text{H}_4\text{COO})_6(\text{phen})_2]$ $n = 2$ (**1**), $n = 4$ (**3**)

The structures of compounds **1** and **3** are shown in Figure 2. Selected bond lengths and angles are listed in Table 1. These structures consist of a linear array of three Mn^{II} ions where the central manganese ion is located on a crystallographic inversion centre. In both compounds, the Mn1 ion is coordinated by six oxygen atoms of six chlorobenzoato

ligands. The Mn1 ion bridges the two terminal Mn2 ions through three chlorobenzoato ligands. Two of them are coordinated through both oxygen atoms ($\mu_{1,3}$), in a *syn-syn* mode, while the third carboxylate bridges through just one oxygen atom ($\mu_{1,1}$), whilst the other oxygen atom (O_d) is weakly bonded to the terminal Mn2 ion. The Mn2-O_d distance is 2.279 and 2.344 Å for compounds **1** and **3**, respectively, which are comparable to those reported in the literature for analogous compounds (2.203–2.823 Å, av. 2.39 Å).^[6–23] The hexacoordination of the terminal Mn2 ion is completed by a 1,10-phenanthroline ligand. The $\text{Mn1}\cdots\text{Mn2}$ distances are 3.630 and 3.546 Å for compounds **1** and **3**, respectively, which agree with those reported in the literature (3.370–3.691 Å).^[6–23]

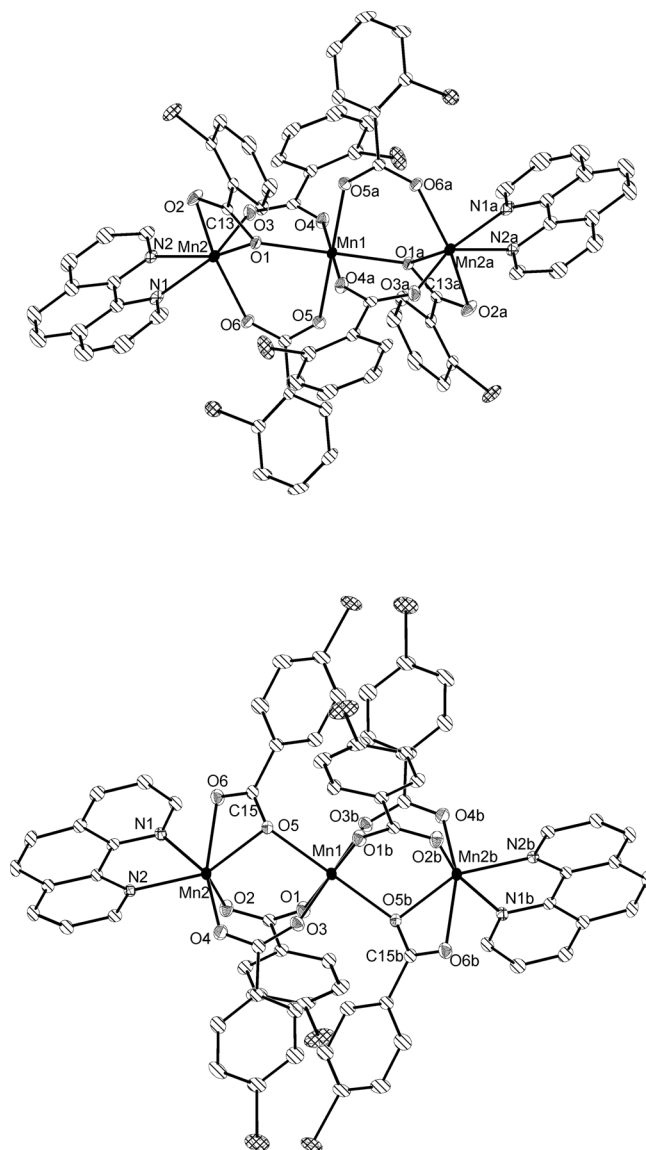


Figure 2. Crystal structures of trinuclear compounds **1** (top) and **3** (bottom) showing the atom labelling scheme. Hydrogen atoms are omitted for clarity.

The Mn1 ion shows a quite regular octahedral environment, although a considerable elongation in the direction of the $\mu_{1,1}$ oxygen bridge (O_b) is observed: the Mn1-O_b dis-

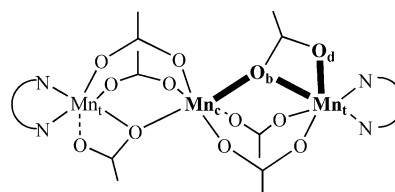
Table 1. Selected bond lengths (Å) and angles (°) with estimated standard deviations in parentheses for trinuclear compounds **1** and **3**·2CH₂Cl₂.^[a]

Compound 1		Compound 3 ·2CH ₂ Cl ₂	
Mn1...Mn2	3.630(0)	Mn1...Mn2	3.546(4)
Mn1–O1	2.2440(16)	Mn1–O5	2.2242(19)
Mn1–O4	2.1627(17)	Mn1–O3	2.1684(19)
Mn1–O5	2.1426(17)	Mn1–O1	2.1273(19)
Mn2–N1	2.275(2)	Mn2–N1	2.301(2)
Mn2–N2	2.266(2)	Mn2–N2	2.234(2)
Mn2–O1	2.2845(16)	Mn2–O5	2.2205(19)
Mn2–O2	2.2787(17)	Mn2–O6	2.344(2)
Mn2–O3	2.0844(18)	Mn2–O2	2.1120(19)
Mn2–O6	2.1029(17)	Mn2–O4	2.109(2)
C13–O1	1.282(3)	C15–O5	1.289(3)
C13–O2	1.244(3)	C15–O6	1.250(3)
Mn2–Mn1–Mn2a	180.00(1)	Mn2–Mn1–Mn2b	179.99(1)
O1–Mn1–O1a	180.00(7)	O5–Mn1–O5b	180.00(8)
O4–Mn1–O4a	180.00(7)	O1–Mn1–O1b	180.00(10)
O5–Mn1–O5a	180.00(7)	O3–Mn1–O3b	180.00(10)
N1–Mn2–O3	162.55(8)	N1–Mn2–O2	160.98(8)
N2–Mn2–O1	157.23(8)	N2–Mn2–O5	156.01(8)
O2–Mn2–O6	148.42(7)	O4–Mn2–O6	156.41(8)
O2–Mn2–O1	57.51(7)	O5–Mn2–O6	57.66(7)
N2–Mn2–N1	73.72(8)	N2–Mn2–N1	73.22(9)

[a] Symmetry codes: (a) $-x, -y, 1-z$, (b) $-x+1, -y, -z+1$.

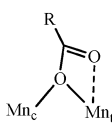
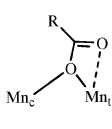
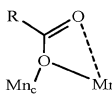
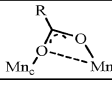
tance is ≈ 2.23 Å, while the other Mn1–O distances are ≈ 2.15 Å. For the Mn2 ions, the acute angles O_d–Mn2–O_b ($\approx 57^\circ$) and N–Mn2–N ($\approx 73^\circ$) and the difference between the Mn2–N (≈ 2.27 Å) and Mn2–O (≈ 2.19 Å) bond lengths lead to a distorted octahedral geometry around the terminal Mn^{II} ions.

These compounds are examples of the *carboxylate shift*, a term used by Lippard to describe the carboxylate movement from $\mu_{1,1}$ -O to $\mu_{1,3}$ -O,O' bridging modes.^[45] Analysis of the structural parameters of this type of compounds containing monodentate bridging carboxylate ligands shows that they can be arranged into three classes, from an absent or a weak Mn_t–O_d interaction (class I) to a strong interaction (class III). However, a further interpretation can be made from bridging and dangling metal-to-oxygen distances (Figure 3). A symmetric bridge is indicative of a strong $\mu_{1,1}$ character, while an asymmetric bridge, with a Mn_t–O_b distance larger than Mn_c–O_b and a short Mn_t–O_d distance, indicate a certain $\mu_{1,3}$ character.

Figure 3. Schematic structure of trinuclear compounds emphasizing the bridging and dangling metal-to-oxygen bonds (in bold) related to the movement from $\mu_{1,1}$ -O to $\mu_{1,3}$ -O,O' bridging modes.

Compound **1** is characterized by an asymmetric $\mu_{1,1}$ -O bridge, with a Mn1–O_b distance (2.244 Å) smaller than the Mn2–O_d and Mn2–O_b distances, which are quite similar (2.285 and 2.279 Å, respectively). This compound therefore shows a bridge intermediate between the $\mu_{1,1}$ and $\mu_{1,3}$ modes, coordinated in a *syn-anti* mode. However, compound **3** shows a Mn1–O_b distance very similar to Mn2–

Table 2. Selected structural parameters and carboxylate bridging mode for trinuclear Mn^{II} compounds with a [Mn₃($\mu_{1,3}$ -RCOO)₄($\mu_{1,1}$ -RCOO)₂] core.

Compound ^[a]	Mn _c –O _b distance / Å	Mn _r –O _b distance / Å	Mn _r –O _d distance / Å	Mn...Mn distance / Å	Carboxylate bridging mode	Ref.
[Mn ₃ (4-ClC ₆ H ₄ COO) ₆ (phen) ₂]·2CH ₂ Cl ₂ (3 ·2CH ₂ Cl ₂)	2.224	2.221	2.344	3.546	 A	this work
[Mn ₃ (C ₆ H ₅ CH=CHCOO) ₆ (bpy) ₂]·H ₂ O	2.221	2.218	2.388	3.527		[7]
[Mn ₃ (2-Boc-C ₆ H ₄ COO) ₆ (dme) ₂]	2.184	2.208	2.366	3.387		[12]
[Mn ₃ (bpy) ₂ [(CH ₃) ₂ CHCOO] ₆]	2.177	2.173	2.471	3.489		[13]
[Mn ₃ (C ₆ H ₅ COO) ₆ (py) ₂ CO–K ⁺ N [–]] ₂	2.214	2.238	2.346	3.552		[23]
[Mn ₃ (2-CNC ₆ H ₄ COO) ₆ (phen) ₂]	2.295	2.282	2.317	3.650		[11]
[Mn ₃ (C ₆ H ₅ COO) ₆ [(ph)(2-py)CO] ₂]	2.240	2.261	2.249	3.603	 B	[14]
[Mn ₃ (CH ₃ COO) ₆ (ppe) ₂] ^[b]	2.245	2.186	2.353	3.596		[10]
[Mn ₃ ((CH ₃) ₂ CHCOO) ₆ (phen) ₂]	2.202	2.167	2.439	3.531		[13]
<i>anti</i> -[Mn ₃ (BIPhMe) ₂ (CH ₃ COO) ₆]·2CH ₂ Cl ₂	2.205	2.172	2.488	3.635		[16]
[Mn ₃ (CH ₃ COO) ₆ (dapdoH ₂) ₂]	2.161	2.193	2.402	3.603		[18]
[Mn ₃ (bpy) ₂ (CH ₃ COO) ₆]	2.202	2.155	2.605	3.614		[19]
[Mn ₃ (CH ₃ COO) ₆ (pybim) ₂]	2.235	2.133	2.823	3.558		[20]
[Mn ₃ (bpy) ₂ (ClCH ₂ COO) ₆]	2.217	2.151	2.611	3.624		[22]
[Mn ₃ (CH ₃ COO) ₆ (phen) ₂]	2.130	2.429	2.354	3.395	 C	[10]
[Mn ₃ (CH ₃ COO) ₆ (L) ₂]	2.197	2.234	2.341	3.643		[6]
[Mn ₃ (bpy) ₂ (FcCOO) ₆]	2.195	2.286	2.358	3.429		[15]
[Mn ₃ (CH ₃ COO) ₆ (phen) ₂]	2.131	2.280	2.422	3.387		[16]
[Mn ₃ [(CH ₃) ₂ CHCOO] ₆ (dpa) ₂]·2CH ₃ CN	2.169	2.218	2.376	3.611	 D	[17]
[Mn ₃ (2-ClC ₆ H ₄ COO) ₆ (phen) ₂] (1)	2.244	2.285	2.279	3.630		this work
[Mn ₃ (bpy) ₂ (C ₆ H ₅ COO) ₆]·H ₂ O	2.251	2.300	2.282	3.588		[9]
[Mn ₃ (C ₆ H ₅ COO) ₆ (py) ₂ CO–K ⁺ N [–] O] ₂]·2CH ₃ CN	2.272	2.322	2.208	3.574		[23]

[a] Abbreviations: Boc = *tert*-butoxycarbonyl; dme = 1,2-dimethoxyethane; BIPhMe = 2,2'-bis(1-methylimidazolyl)phenylmethoxymethane; dapdoH₂ = 2,6-diacetylpyridine dioxime; (py)₂CO = di-2-pyridyl ketone; (ph)(2-py)CO = phenyl 2-pyridyl ketone; ppei = 2-pyridinal-1-phenylethylamine; pybim = 2-(2-pyridyl)benzimidazole; L = bis(1-methylimidazol-2-yl)methanone; dpa = 2,2'-dipyridylamine. [b] One of the two crystallographically independent molecules present in the unit cell.

O_b (2.221 and 2.224 Å, respectively) and smaller than Mn2–O_d (2.344 Å). In this case, the bridge shows a significant $\mu_{1,1}$ character.

Table 2 presents some structural parameters of trinuclear compounds analogous to those reported here and the $\mu_{1,1}$ or $\mu_{1,3}$ character of the carboxylate bridge. All these compounds can be arranged into four classes. Class A compounds show a quite symmetric bridge (pronounced $\mu_{1,1}$ character) and a medium Mn_t–O_d interaction, although there are two compounds with a strong Mn_t–O_d interaction, the three distances being of the same order of magnitude.^[11,14] The other three classes show asymmetric bridges. In class B, the bridge is displaced towards Mn_t, and the Mn_t–O_d interaction is very weak. Class C collects compounds with the bridge displaced towards Mn_c, with a rather short Mn_c–O_b distance and a large Mn_t–O_d distance. However, the compound [Mn₃(CH₃COO)₆(phen)₂] shows a larger Mn_t–O_b distance than the other compounds of this group.^[10] Compounds in class D, which are very scarce, display the bridge shifted also towards Mn_c, but with the Mn_c–O_b distance a bit larger than those in compounds of class C, and a short Mn_t–O_d distance (even shorter than Mn_t–O_b), showing a bridging mode with strong $\mu_{1,3}$ character. Comparison of the Mn···Mn distance for the different classes shows slightly smaller values for compounds in class A and for some in class C, but the differences are not very significant.

[Mn(μ -3-ClC₆H₄COO)₂(phen)]_n (4)

The structure of **4** consists of an infinite zigzag Mn^{II} chain, as shown in Figure 4. Selected bond lengths and angles are given in Table 3. Each manganese ion coordinates four chlorobenzoato ligands and one 1,10-phenanthroline, displaying a distorted octahedral geometry. The manganese ions are bridged by two carboxylate ligands coordinated in a *syn-anti* mode, with a Mn···Mn distance of 4.546 Å, which is slightly longer than that reported for the analogous compound with 2,2'-bipyridine (4.515 Å)^[21] but in the range of distances reported for other 1D compounds with a [Mn($\mu_{1,3}$ -RCOO)₂]_n core (4.515–4.852 Å).^[21,22,24–33] There are two different Mn–O distances: the shortest distances (2.091 Å) correspond to O_{syn}, while the largest distances (2.200 Å) correspond to O_{anti}. The O_{syn} atoms are *trans* to a N_{phen} atom, while the O_{anti} atoms are *trans* to the other O_{anti} atoms. The Mn–O_{syn} distance is shorter than the Mn–O_{anti} distance, which is also observed in analogous compounds with a *syn-anti* coordination mode of the carboxylate bridge, where the Mn–O_{syn} distance is in the range 2.077–2.145 Å and the Mn–O_{anti} distance is in the range 2.183–2.238 Å.^[21,22,26–33] The two Mn–N distances are 2.298 Å, which agree with those in the literature, which fall in the range 2.252–2.310 Å.^[21,22,26–33]

The phenanthroline rings are parallel to each other along the 1D chain, with a distance of 7.221 Å between them. The phen ligands of neighbouring polymeric chains are arranged in an almost parallel fashion, and the angle is 2.11°.

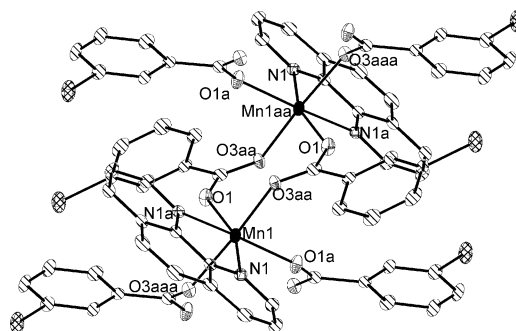


Figure 4. Crystal structure of the 1D compound **4**, showing a dinuclear fragment with the atom labelling scheme. Hydrogen atoms are omitted for clarity.

Table 3. Selected bond lengths (Å) and angles (°) with estimated standard deviations in parentheses for the 1D compound **4**.^[a]

Mn1···Mn1aa	4.546(1)	N1a–Mn1–O1a	158.46(8)
Mn1–O1	2.0908(18)	O1–Mn1–N1	158.46(8)
Mn1–N1	2.298(2)	O3aa–Mn1–O3aaa	167.39(9)
Mn1–O3aa	2.2004(18)		

[a] Symmetry codes: (a) $-x + 1, y, -z + 1/2$; (aa) $-x + 1, -y, -z + 1$; (aaa) $x, -y, z - 1/2$.

The face-to-face distance between two phen ligands of adjacent chains is 3.306 Å. This suggests π – π stacking interactions between polymeric chains (Figure 5).

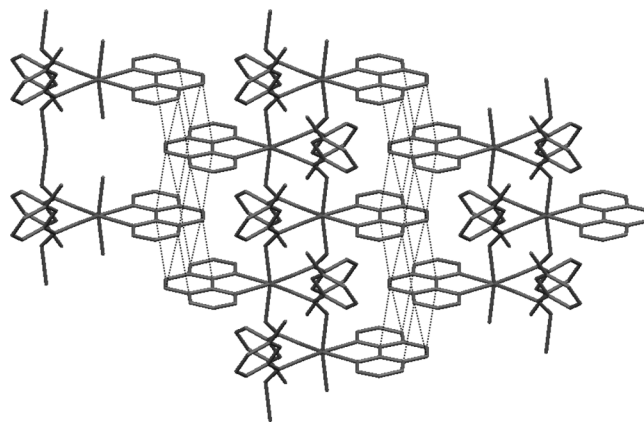


Figure 5. Interaction between neighbouring chains through the phen ligands, view along the *a* axis.

[{Mn(4-ClC₆H₄COO)(phen)}₂(μ -4-ClC₆H₄COO)₂(μ -H₂O)] (5)

The structure of this neutral dinuclear compound is shown in Figure 6. Selected bond lengths and angles are listed in Table 4. The Mn^{II} ions are bridged by one H₂O molecule and two $\mu_{1,3}$ -chlorobenzoato ligands, in a *syn-anti* mode. The hexacoordination of each manganese ion is completed by a phen ligand and a monodentate chlorobenzoato ligand. The molecular conformation is stabilized by hydrogen bonds between the non-coordinated oxygen atom of the monodentate carboxylate group and the hydrogen atoms of the bridging water molecule.

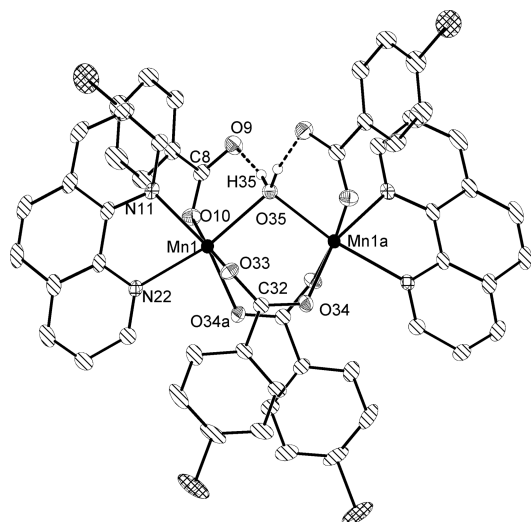


Figure 6. Crystal structure of neutral dinuclear compound **5** showing the atom labelling scheme. Hydrogen atoms (except those of the water bridge) are omitted for clarity.

Table 4. Selected bond lengths (Å) and angles (°) with estimated standard deviations in parentheses for the neutral dinuclear compound **5**.^[a]

Mn1...Mn1a	3.484(7)	C8–O10	1.262(3)
Mn1–O34a	2.1422(14)	C32–O34	1.260(2)
Mn1–O10	2.1617(15)	C32–O33	1.263(2)
Mn1–O33	2.1824(14)	O35–H35	0.92(3)
Mn1–O35	2.2428(14)	O35–Mn1–N22	162.09(5)
Mn1–N11	2.2952(17)	O34a–Mn1–N11	160.72(6)
Mn1–N22	2.2622(17)	O10–Mn1–O33	174.51(6)
C8–O9	1.252(3)	Mn1–O35–Mn1a	101.94(8)

[a] Symmetry codes: (a) $-x + 3/2, y, -z + 1$.

The Mn...Mn distance is 3.484 Å, the shortest distance found for this type of compound (3.502–3.786 Å).^[34–44] The Mn–O_w–Mn angle (101.84°) is also one of the smallest values reported in the literature (101.70–114.97°). However, the Mn–O_w distance of 2.243 Å agrees with those in the literature that fall in the range 2.111–2.315 Å. The distances between the manganese ions and the oxygen atoms of the carboxylate bridges are quite different: the Mn1–O34 distance is shorter than Mn1–O33 (2.142 and 2.182 Å, respectively), probably because of the *trans* effect. With regard to the monodentate carboxylate, the C8–O9 distance is similar to the C8–O10 distance, which indicates a significant delocalization of the double bond as a result of the hydrogen bond between the non-coordinated oxygen atom and the bridging water molecule (H35–O9 distance of 1.643 Å).

Magnetic Measurements

Magnetic susceptibility data were recorded for all compounds (**1–5**), from room temperature to 2 K. $\chi_M T$ vs. T and M vs. H plots for trinuclear compounds **1–3** are shown in Figure 7. The three compounds show analogous magnetic behaviour. At 300 K, the $\chi_M T$ values are 13.20, 13.51 and 13.85 cm³ mol^{−1} K for compounds **1**, **2** and **3**, respec-

tively, close to the value of 13.125 cm³ mol^{−1} K, which corresponds to three uncoupled Mn^{II} ions. When the temperature decreases, the $\chi_M T$ values fall until reaching 4.58 (**1**), 4.46 (**2**) and 4.27 cm³ mol^{−1} K (**3**) at 2 K, which are very close to the expected value of 4.375 cm³ mol^{−1} K for a spin ground state $S_T = 5/2$ and $g = 2$, indicative of an antiferromagnetic coupling. This spin value is confirmed by the field dependence of the magnetization at 2 K, which shows a $M/N\beta$ value indicative of five unpaired electrons (inset Figure 7).

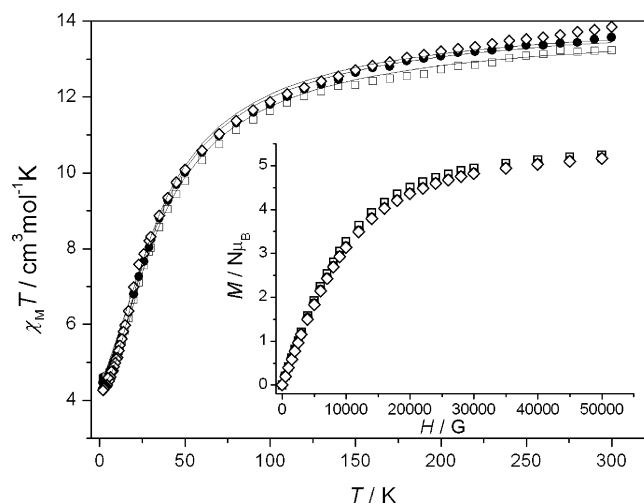
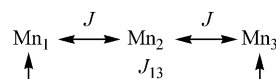


Figure 7. $\chi_M T$ vs. T and M vs. H (inset) plots for [Mn₃(μ-*n*-ClC₆H₄COO)₆(phen)₂] ($n = 2, 3, 4$) **1** (□), **2** (●), **3** (◇). The solid line is the best fit to the experimental data.

On the basis of the structure of these compounds and Kambe's vector coupling scheme (Scheme 1),^[46] the spin Hamiltonian considered would be $H = -J(S_1 \cdot S_2 + S_2 \cdot S_3) - J_{13}(S_1 \cdot S_3)$, where it is assumed that $J_{12} = J_{13} = J$. However, because of the large distance between the terminal manganese ions in the linear complex, Mn₁...Mn₃, their magnetic interaction is negligible ($J_{13} = 0$)^[19,21] and only the Mn₁...Mn₂ and Mn₂...Mn₃ interactions (J) are considered. The expression for the magnetic susceptibility of three linear Mn^{II} ions is obtained from the Van Vleck formula.^[47] The best fit of experimental data corresponds to $J = -2.9$ cm^{−1}, $g = 2.02$, and $R = 2.18 \times 10^{-4}$ for compound **1**, $J = -2.8$ cm^{−1}, $g = 2.03$ and $R = 1.04 \times 10^{-4}$ for compound **2** and $J = -2.8$ cm^{−1}, $g = 2.04$ and $R = 2.48 \times 10^{-4}$ for compound **3**. These J values agree with those from −5.6 to −2.1 cm^{−1} reported in the literature for other linear Mn^{II} trinuclear compounds.^[15–22]



Scheme 1. Kambe's vector coupling scheme.^[46]

Selected structural parameters and J values of compounds **1** and **3** as well as those of some other analogous Mn^{II} compounds reported are listed in Table 5. For trinuclear complexes, the μ_{1,3}-carboxylate bridges are coordinated in a *syn-syn* mode and the oxo bridge is formed by a

Table 5. Selected structural and magnetic data for Mn^{II} compounds with a [Mn₃(μ_{1,3}-RCOO)₄(μ_{1,1}-RCOO)₂] core.

Compound ^[a]	Class	Mn···Mn / Å	Mn–O _b ^[b] / Å	Mn–O _d / Å	(Mn–O _d) – (Mn–O _b) / Å	Mn–O _b –Mn / °	<i>J</i> ^[c] / cm ^{−1}	Ref.
[Mn ₃ (bpy) ₂ (FcCOO) ₆]	C	3.429	2.241	2.358	0.117	99.82	−4.8	[15]
[Mn ₃ ((CH ₃) ₂ CHCOO) ₆ (dpa) ₂]·2CH ₃ CN	C	3.611	2.194	2.376	0.182	110.82	−3.7	[17]
[Mn ₃ (bpy) ₂ (CH ₃ COO) ₆]	B	3.614	2.179	2.605	0.426	112.12	−4.4	[19]
[Mn ₃ (bpy) ₂ (ClCH ₂ COO) ₆]	B	3.624	2.184	2.611	0.427	112.12	−3.8	[22]
[Mn ₃ (CH ₃ COO) ₆ (pybim) ₂]	B	3.558	2.184	2.823	0.639	109.07	−3.6	[20]
[Mn ₃ {(CH ₃) ₂ CHCOO} ₆ (phen) ₂]	B	3.531	2.185	2.439	0.254	107.85	−3.2	[13]
[Mn ₃ (CH ₃ COO) ₆ (dapdoH ₂) ₂]	B	3.603	2.177	2.402	0.225	111.7	−3.2	[18]
[Mn ₃ (bpy) ₂ {(CH ₃) ₂ CHCOO} ₆]	A	3.489	2.175	2.471	0.296	106.67	−3.7	[13]
[Mn ₃ (4-ClC ₆ H ₄ COO) ₆ (phen) ₂] (3·2CH ₂ Cl ₂)	A	3.546	2.223	2.344	0.121	105.82	−2.8	this work
[Mn ₃ (C ₆ H ₅ COO) ₆ {(ph)(2-py)CO} ₂]	A	3.603	2.251	2.249	−0.002	106.31	−2.7	[14]
[Mn ₃ (2-ClC ₆ H ₄ COO) ₆ (phen) ₂] (1)	D	3.630	2.265	2.279	0.014	106.58	−2.9	this work
[Mn ₃ (BIPhMe) ₂ (CH ₃ COO) ₆] ^[d]	–	3.597	2.230	2.419	0.109	109.8	−5.6	[16]

[a] Abbreviations: BIPhMe = 2,2'-bis(1-methylimidazolyl)phenylmethoxymethane; Fc = ferrocene; dpa = 2,2'-dipyridylamine; pybim = 2-(2-pyridyl)benzimidazole; dapdoH₂ = 2,6-diacetylpyridine dioxime; (py)₂CO = di-2-pyridyl ketone; (ph)(2-py)CO = phenyl 2-pyridyl ketone. [b] Average value for Mn_c–O_b and Mn_t–O_b distances. [c] Magnetic exchange coupling parameter based on the Hamiltonian $H = -J(S_1 \cdot S_2 + S_2 \cdot S_3)$. [d] Structural data are average values for all three isomers of [Mn₃(BIPhMe)₂(CH₃COO)₆] as magnetic data are available for a bulk sample possibly containing all three isomers.

μ_{1,1}-carboxylate ligand, where the Mn–O_b distance is in the range between 2.175 and 2.265 Å and the Mn–O_b–Mn angle between 99.82 and 112.2°. As was reported for Cu^{II} compounds,^[48] the magnetic interaction is very sensitive to the M–O_b–M angle and is more antiferromagnetic for larger angles. Therefore, in this type of compounds, the antiferromagnetic interaction may depend on the Mn–O_b–Mn angle. However, there are other factors, such as the μ_{1,1} or μ_{1,3} character of the monatomic bridge, which may provide different pathways for the magnetic interaction. For compounds in class A, the interaction through the μ_{1,1} bridge should be the most important pathway for the magnetic interaction, although some small contribution from the μ_{1,3} pathway may exist. For compounds of classes B and C, the most important pathway for the magnetic interaction is the μ_{1,1} bridge. On the other hand, for compounds of class D, both pathways, μ_{1,1} and μ_{1,3}, may contribute to the magnetic coupling.

By taking into account this classification, although there are few compounds in class C (two) and D (only one), a slight trend may be observed with respect to the $|J|$ value: $|J|_C > |J|_B > |J|_A > |J|_D$. Compounds with the additional μ_{1,3} pathway show a weaker antiferromagnetic coupling than compounds in which the interaction is mediated only through the μ_{1,1} bridge. Therefore, the extra μ_{1,3} pathway decreases the antiferromagnetic interaction. The difference between the Mn_t–O_d and Mn_{c/t}–O_b distances (Δ) could express the μ_{1,1} character (high values of Δ) or the μ_{1,1} + μ_{1,3} character (low values of Δ) of the bridge. A certain correlation between Δ and J can be observed (Figure 8).

However, there are three compounds that do not obey this tendency. One of them is [Mn₃(BIPhMe)₂(CH₃COO)₆]; in this case, the magnetic data corresponds to a bulk sample that may possibly contain the three different isomers found for this compound. In the case of [Mn₃(bpy)₂(FcCOO)₆], the deviation may be due to the ferrocene group in the carboxylate bridge, which is not comparable with the other

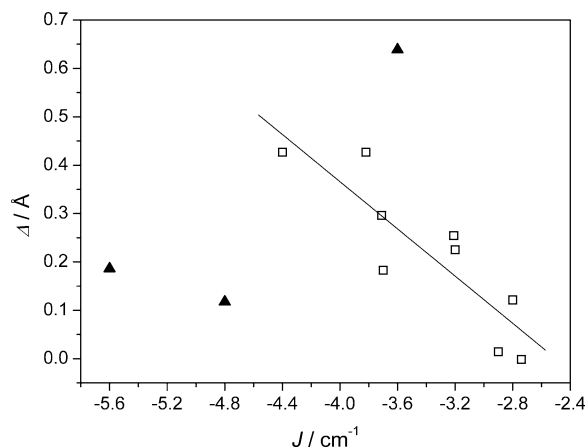


Figure 8. Trend observed between the J value and the difference between Mn_t–O_d and Mn–O_b distances (Δ) in trinuclear compounds. ▲ corresponds to compounds that are not considered (see text).

substituents. The last exception is [Mn₃(CH₃COO)₆(pybim)₂], which displays a Mn–O_d distance (2.823 Å) that is much larger than those in the other compounds. In spite of these exceptions, a linear correlation between Δ and J is observed: the larger the difference (Δ), the more antiferromagnetic the compound. However, there may be some other factors contributing to the magnetic coupling in these compounds.

For the 1D compound **4**, $\chi_M T$ values decrease from 4.50 cm³ mol^{−1} K at 300 K, close to the typical value for one Mn^{II} ion (4.375 cm³ mol^{−1} K), to 0.19 cm³ mol^{−1} K at 2 K, showing an antiferromagnetic interaction between the manganese ions in the chain (Figure 9). The magnetic susceptibility data were analyzed by the analytical expression derived by Fisher^[49] for an infinite chain of classical spins based on the Hamiltonian $H = -J\sum S_i \cdot S_{i+1}$, for local spin values of $S = 5/2$. The best fit is obtained with $J = -1.8$ cm^{−1}, $g = 2.07$ and $R = 6.57 \times 10^{-5}$.

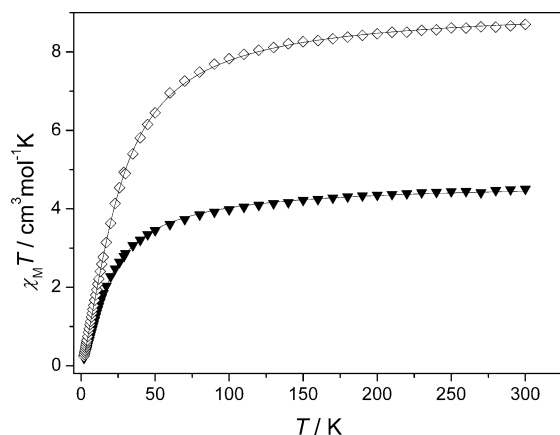


Figure 9. $\chi_M T$ vs. T plot for $[\text{Mn}(\mu\text{-3-ClC}_6\text{H}_4\text{COO})_2(\text{phen})]_n$ (**4**, \blacktriangledown) and $[\{\text{Mn}(4\text{-ClC}_6\text{H}_4\text{COO})(\text{phen})\}_2(\mu\text{-4-ClC}_6\text{H}_4\text{COO})_2(\mu\text{-H}_2\text{O})]$ (**5**, \diamond). The solid line is the best fit to the experimental data.

To the best of our knowledge, there are only three 1D compounds with a similar core that have been structurally and magnetically characterized.^[21,22,24] As can be seen in Table 6, the analogous compound with a bpy ligand, $[\text{Mn}(\text{bpy})(3\text{-ClC}_6\text{H}_4\text{COO})_2]_n$ ^[21] shows similar structural parameters and J value to those of **4**, which is indicative of the minor effect of the basicity of the terminal ligands. However, changing the bridging ligands from chlorobenzoato to chloroacetato as in $[\text{Mn}(\text{ClCH}_2\text{COO})_2(\text{phen})]_n$ ^[22] leads to a modification of the Mn–O distances and hence the J value. In these compounds, the carboxylate bridging ligands are coordinated in a *syn-anti* mode, with a Mn–O_{syn} distance shorter than the Mn–O_{anti} distance. The difference between these distances is smaller for the chloroacetato compound than for the chlorobenzoato compounds, and its magnetic interaction is weaker than for compound **4** and the analogous compound with bpy.^[21] A larger antiferromagnetic coupling was reported for $[\text{Mn}(\text{FcC}_6\text{H}_4\text{COO})_2(\text{phen})]_n$ ^[24] in which the carboxylate

bridges are coordinated in a *syn-syn* mode. Moreover, the difference between the two Mn–O distances in this compound is larger than for the other compounds. Both factors could explain the larger $|J|$ value reported for this chain.^[50]

The dinuclear compound **5** shows a $\chi_M T$ value of $8.70 \text{ cm}^3 \text{ mol}^{-1} \text{ K}$ at 300 K, which is very close to the expected value for two uncoupled Mn^{II} ions ($8.75 \text{ cm}^3 \text{ mol}^{-1} \text{ K}$) (Figure 9). On decreasing the temperature, the $\chi_M T$ values fall until $0.24 \text{ cm}^3 \text{ mol}^{-1} \text{ K}$, indicative of an antiferromagnetic coupling. The experimental data were fitted by using the spin Hamiltonian $H = -J S_1 \cdot S_2$ and the corresponding susceptibility expression for two Mn^{II} ions,^[47] obtaining the best fit with $J = -3.6 \text{ cm}^{-1}$, $g = 2.05$ and $R = 3.52 \times 10^{-5}$. This J value agrees with those reported in the literature, from -5.8 to -2.0 cm^{-1} (Table 7).^[41–44] All magnetically studied compounds show that the carboxylate bridging ligands are coordinated in a *syn-syn* mode. However, compound **5** displays a *syn-anti* coordination mode, with Mn–O_{syn} distances shorter than Mn–O_{anti} distances, and it shows the shortest Mn···Mn distance and the smallest Mn–O_b–Mn angle.

The five compounds reported here (**1–5**) show an antiferromagnetic behaviour; the $|J|$ values decrease from the neutral dinuclear compound to the 1D system, $|J|_{\text{di}} > |J|_{\text{tri}} > |J|_{\text{1D}}$, the magnetic coupling constant for the 1D system (**4**) being appreciably smaller. In this compound, the magnetic interaction is through two $\mu_{1,3}$ -carboxylate bridging ligands, while in the dinuclear and trinuclear complexes there is an additional monatomic bridge: an oxygen atom from a $\mu_{1,1}$ -carboxylate ligand for the trinuclear compounds (**1** and **3**) or from a $\mu\text{-H}_2\text{O}$ ligand for the dinuclear compound (**5**) (Scheme 2). On the other hand, the $\mu_{1,3}$ -carboxylate bridging ligand can be coordinated in a *syn-syn* mode, as in **1** and **3**, or in a *syn-anti* mode, as in **4** and **5**. It is well known that the magnetic interaction through the $\mu_{1,3}$ -carboxylate bridging ligand is usually weak and antiferromagnetic, and depends on the coordination mode of the carboxylate li-

Table 6. Selected structural and magnetic data for Mn^{II} 1D systems $[\text{Mn}(\mu\text{-RCOO})_2(nm)]_n$.

Compound ^[a]	Mn–O _{syn} / Å	Mn–O _{syn/anti} / Å	$J^{[b]}$ / cm ^{−1}	Ref.
$[\text{Mn}(3\text{-ClC}_6\text{H}_4\text{COO})_2(\text{phen})]_n$ (4)	2.091	2.200 _{anti}	−1.8	this work
$[\text{Mn}(\text{bpy})(3\text{-ClC}_6\text{H}_4\text{COO})_2]_n$	2.104	2.196 _{anti}	−1.7	[21]
$[\text{Mn}(\text{ClCH}_2\text{COO})_2(\text{phen})]_n$	2.134	2.183 _{anti}	−0.9	[22]
$[\text{Mn}(\text{FcC}_6\text{H}_4\text{COO})_2(\text{phen})]_n$	2.090 ^c	2.210 _{syn} ^[c]	−6.5	[24]

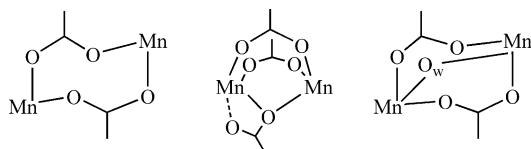
[a] Abbreviations: Fc = ferrocene. [b] Magnetic exchange coupling parameter based on the Hamiltonian $H = -JS_1 \cdot S_{i+1}$. [c] Average values.

Table 7. Selected structural and magnetic data for Mn^{II} dinuclear compounds with a $[\text{Mn}_2(\mu\text{-RCOO})_2(\mu\text{-H}_2\text{O})]^{2+}$ core.

Compound ^[a]	Mn···Mn / Å	Mn–O _{syn} / Å	Mn–O _{syn/anti} / Å	Mn–O _b / Å	Mn–O _b –Mn / °	$J^{[b]}$ / cm ^{−1}	Ref.
$[\text{Mn}_2(\text{F}_3\text{C}_2\text{COO})_4(\text{H}_2\text{O})_3\text{L}_2]$	3.739	2.115 ^[c]	2.152 _{syn} ^[c]	2.252 ^[c]	114.6	−3.3	[41]
$[\text{Mn}_2(\text{CH}_3\text{COO})_4(\text{H}_2\text{O})(\text{tmeda})_2]$	3.621	2.136 ^[c]	2.127 _{syn} ^[c]	2.210 ^[c]	110.04	−5.8	[42]
$[\text{Mn}_2(\text{H}_2\text{O})(\text{Me}_2\text{bpy})_2(\text{piv})_4]$	3.595	2.109 ^[c]	2.163 _{syn} ^[c]	2.192 ^[c]	110.16	−5.5	[42]
$[\text{Mn}_2(\text{CH}_3\text{COO})_4(\text{H}_2\text{O})_2(\text{im})_4]$	3.777	2.206	2.183 _{syn}	2.227	114.4	−2.5	[43]
$[\text{Mn}_2(\text{CH}_3\text{COO})_5(\text{H}_2\text{O})(\text{py})_4]$	3.618	2.144 ^[c]	2.140 _{syn} ^[c]	2.182 ^[c]	108.3	−2.0	[44]
$[\text{Mn}_2(4\text{-ClC}_6\text{H}_4\text{COO})_4(\text{H}_2\text{O})(\text{phen})_2]$ (5)	3.484	2.142	2.182 _{anti}	2.243	101.94	−3.6	this work

[a] Abbreviations: L = 2-ethyl-4,4',5,5'-tetramethyl-3-oxo-4,5-dihydro-1H-imidazolyl-1-oxyl; tmeda = *N,N,N',N'*-tetramethylethylenediamine; piv = pivalate; Me₂bpy = 4,4'-dimethyl-2,2'-bipyridine; im = imidazole; py = pyridine. [b] Magnetic exchange coupling parameter based on the Hamiltonian $H = -JS_1 \cdot S_2$. [c] Average values.

gand: the *syn-syn* mode induces larger $|J|$ values than the *syn-anti* mode.^[50] The presence of a monatomic bridge in the dinuclear and trinuclear complexes reduces the Mn...Mn distance and increases the $|J|$ value, displaying a major antiferromagnetic coupling. Therefore, both factors can influence the magnetic exchange interaction.



Scheme 2. Bridges found in 1D, trinuclear and dinuclear compounds reported in this study, respectively.

It is interesting to compare the two compounds with the same $\mu_{1,3}$ -carboxylate ligand, 4-ClC₆H₄COO, and one oxygen-bridging ligand (**3** and **5**). This monatomic ligand must be the most important pathway for the antiferromagnetic interaction. As was indicated, this interaction is very sensitive to the M–O_b–M angle, and is more antiferromagnetic for larger angle values. Compound **3** presents a larger angle than compound **5** (105.82 and 101.94°, respectively) and $\mu_{1,3}$ -carboxylate ligands in a *syn-syn* mode, compared to a *syn-anti* mode in compound **5**. A greater antiferromagnetic behaviour should therefore be expected for **3** than for **5**. However, the experimental results show a larger $|J|$ value for **5** than for **3**. In the trinuclear complex, one of the carboxylate ligands coordinated in a *syn-syn* mode is coplanar to the Mn–O_b–Mn group and could exert a countercomplementary effect, so would decrease the antiferromagnetic contribution through the oxo bridge.^[48] Therefore, the $|J|$ value is less than that expected, and this effect could explain the greatest antiferromagnetic behaviour found for compound **5**.

EPR Spectra

The EPR spectra of compounds **1–5** were recorded on powdered samples at different temperatures. At room temperature, all of them show a band centred at $g \approx 2$; however, at 4 K, the spectrum of each compound is noticeably different and allows identification of each type of complex.

The shape of the spectra of the trinuclear compounds **1–3** is very sensitive to temperature. A very broad band centred at $g \approx 2$ is observed at 295 K, with a peak-to-peak linewidth (ΔH_{pp}) of 930 G for **1**, 890 G for **2** and 860 G for **3**. A broadening of this band is observed by decreasing the temperature until 100 K, where the ΔH_{pp} is 960 G for **1**, 995 G for **2** and 950 G for **3**. This band remains the most intense feature until very low temperatures. However, at 4 K, the spectrum becomes quite complicated: the most intense signal is found at low field ($g \approx 4$), with a less intense signal at $g \approx 2$ and some others at high field. Figure 10 shows the effect of temperature on the EPR spectrum of compound **3**; a similar behaviour is observed for the other two trinuclear complexes (**1** and **2**). This spectrum is characteristic of this type of compound.^[19–23] As was indicated,

the ground state is $S_T = 5/2$ with $S_{13} = 5$, and the first excited state ($S_T = 3/2$ with $S_{13} = 4$) is at $-3J/2$ above the ground state. Therefore, when $J \approx -2.8 \text{ cm}^{-1}$, at 4 K only the ground state may be populated. A spin state $S_T = 5/2$ can exhibit zero-field splitting (ZFS), which causes three doubly degenerate spin states, $M_s = \pm 1/2, \pm 3/2$ and $\pm 5/2$ (Kramer's degeneracy). If the ZFS effect is negligible, a narrow signal may arise around $g = 2$; however, when the ZFS is considerable, the signal should be broad at room temperature and split into several features at low temperature, as found for compounds **1–3** and for analogous compounds reported in the literature.^[19–22]

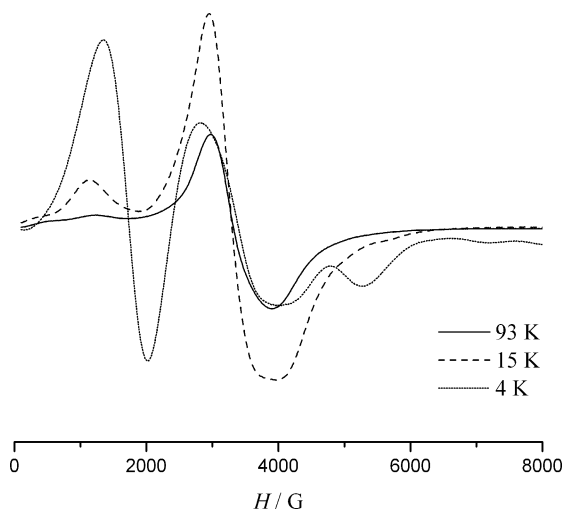


Figure 10. Variable-temperature X-band EPR spectra of a powdered sample of trinuclear compound **3**.

The spectra at 4 K were simulated, with the easyspin software,^[51] by considering an isolated spin state $S = 5/2$ with axial (D) and rhombic (E) zero-field splitting. The ZFS parameters obtained from these simulations therefore correspond to the ground state, $D_{5/2}$ and $E_{5/2}$ and depend on the ZFS parameters of the interacting ions, D_{Mn} and E_{Mn} , and dipolar and anisotropic interactions between the ions. By using this approach, quite good simulations were obtained with $D_{5/2} = 0.16 \text{ cm}^{-1}$ and $E_{5/2} = 0.05 \text{ cm}^{-1}$ (linewidth of 600 G) for compound **1**, $D_{5/2} = 0.16 \text{ cm}^{-1}$ and $E_{5/2} = 0.043 \text{ cm}^{-1}$ (linewidth of 450 G) for compound **2** and $D_{5/2} = 0.16 \text{ cm}^{-1}$ and $E_{5/2} = 0.053 \text{ cm}^{-1}$ (linewidth of 800 G) for compound **3** (Figure 11). These simulations reproduce the bands at low field quite well. However, compounds **1** and **3** show other features around $g < 2$ that are not possible to reproduce with similar ZFS values to compound **2**. Nevertheless, D and E values obtained for these compounds are comparable to those reported elsewhere.^[22]

The EPR spectrum of the 1D system **4** shows a single band centred at $g \approx 2$ that widens on decreasing the temperature (Supporting Information, Figure S1). The peak-to-peak linewidth changes from 98 G at 77 K to 147 G at 4 K. The same behaviour was observed for analogous compounds reported in the literature.^[21,22] This broadening on lowering the temperature may be explained by considering the main factors that influence the linewidth for an iso-

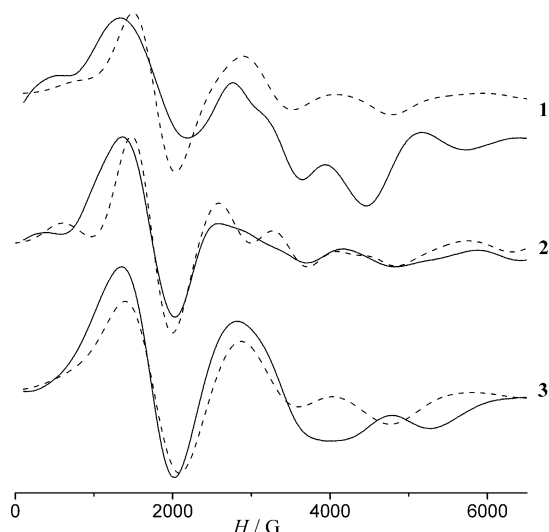


Figure 11. X-band EPR spectra of powdered samples of trinuclear compounds 1–3 at 4 K. The dashed line is the best simulation achieved.

tropic Heisenberg 1D system.^[52] When the superexchange interactions along the chain are the predominant effect, a narrowing of the signal is observed, while when the dipolar interactions are more important, a broadening of the signal is observed, as in compound 4. Moreover, for Mn^{II} 1D systems, there are additional broadening mechanisms, such as the hyperfine coupling and the single-ion ZFS effects.

Neutral dinuclear compound 5 also displays some changes in the shape of the EPR spectrum at different temperatures (Supporting Information, Figure S2). The most important signal, centred at $g \approx 2$, shows a ΔH_{pp} of 260 G at 77 K, which increases until reaching 360 G at 4 K. This compound shows an antiferromagnetic coupling, the ground state is therefore $S = 0$, and at 4 K it should be EPR-silent. However, as the J value is small (-3.6 cm^{-1}), the lowest excited states may also be populated.

For the simulation of the experimental EPR spectrum at 4 K with the easyspin software,^[51] a dinuclear system of two $S = 5/2$ ions was considered, with a magnetic exchange in-

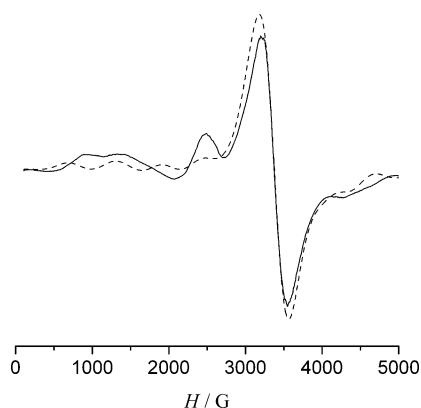


Figure 12. X-band EPR spectra of powdered sample of neutral dinuclear compound 5. The dashed line is the best simulation achieved.

teraction $J = -3.6 \text{ cm}^{-1}$ and the zero-field splitting parameters of the single ion D_{Mn} and E_{Mn} . A fairly good simulation was obtained with $D_{\text{Mn}} = 0.187 \text{ cm}^{-1}$ and $E_{\text{Mn}} = 0.061 \text{ cm}^{-1}$ and $g = 2$ (Figure 12).

Conclusions

The three chlorobenzoato ligands (*ortho*, *meta* and *para*) behave differently when forming polynuclear Mn^{II} compounds. Depending on the Mn^{II} /phen ratio or solvent, three types of complexes were obtained. For 2- $\text{ClC}_6\text{H}_4\text{COO}$, independent of the ratio or solvent, only the trinuclear complex 1 was obtained. With 3- $\text{ClC}_6\text{H}_4\text{COO}$, independent of the solvent, two compounds were obtained: the trinuclear complex 2 and the 1D system 4. For 4- $\text{ClC}_6\text{H}_4\text{COO}$, independent of the Mn^{II} /phen ratio, trinuclear 3 and the neutral dinuclear compound 5 were obtained when ethanol and acetonitrile were used, respectively.

The five compounds were magnetically characterized, all displaying weak antiferromagnetic coupling. The exchange coupling depends on the number of bridges involved and the carboxylate bridge conformation. The dinuclear and trinuclear compounds, with three bridging ligands, present $|J|$ values of the same order and larger than that of the 1D compound, which has only two bridging ligands. In the trinuclear complexes, the countercomplementary effect of the $\mu_{1,3}$ -carboxylate bridges reduces the antiferromagnetic interaction. It is possible to distinguish the different compounds from their EPR spectrum at 4 K.

Experimental Section

General Remarks: C, H, N and Cl analyses were carried out by the Servei de Microanàlisi of the Consell Superior d'Investigacions Científiques (CSIC). Infrared spectra were recorded on KBr pellets in the range 4000–400 cm^{-1} with a Thermo Nicolet Avatar 330 FTIR spectrometer. X-ray diffraction measurements and resolution were carried out at the Unidade de Raios X (Universidade de Santiago de Compostela). Magnetic susceptibility measurements (2–300 K) and magnetization measurements at 2 K, (0–50000 G) were carried out in a Quantum Design MPMP SQUID Magnetometer at the Unitat de Mesures Magnètiques (Universitat de Barcelona). Two different magnetic fields were used for the susceptibility measurements, 300 G (2–5 K) and 3000 G (2–300 K), with superimposable graphs. Pascal's constants were used to estimate the diamagnetic corrections for the compound. The fit was performed by minimising the function $R = \sum[(\chi_{\text{M}}T)_{\text{exp}} - (\chi_{\text{M}}T)_{\text{calcd}}]^2 / \sum[(\chi_{\text{M}}T)_{\text{exp}}]^2$. Solid-state EPR spectra were recorded with X-band (9.4 GHz) frequency from room temperature to 4 K by using a Bruker ESP-300E spectrometer, at the Unitat de Mesures Magnètiques (Universitat de Barcelona). The computational package easyspin^[51] was used to simulate the EPR spectra of the trinuclear and dinuclear compounds. For the trinuclear complexes, the simulation was performed by considering an isolated ground state, $S = 5/2$, with zero-field splitting (D and E). The simulation of the EPR spectrum of the dinuclear complex was performed by considering all the spin states and including the magnetic interaction between the Mn^{II} ions (J) and the zero-field splitting parameters for each manganese ion (D_{Mn} and E_{Mn}) in the calculations.

Synthesis: All manipulations were carried out at room temperature under aerobic conditions. Reagents and solvents were obtained from commercial sources and used without further purification. $[\text{Mn}(n\text{-ClC}_6\text{H}_4\text{COO})_2] \cdot n\text{H}_2\text{O}$ ($n = 2, 3, 4$) was synthesized by the reaction of MnCO_3 and $n\text{-ClC}_6\text{H}_4\text{COOH}$ in boiling water. After several hours, the solution was filtered and concentrated under reduced pressure to give a pale pink precipitate of the desired product. Yields were calculated from the stoichiometric reaction.

Synthesis of Compounds

$[\text{Mn}_3(\mu\text{-}2\text{-ClC}_6\text{H}_4\text{COO})_6(\text{phen})_2]$ (1): $[\text{Mn}(2\text{-ClC}_6\text{H}_4\text{COO})_2] \cdot n\text{H}_2\text{O}$ (0.60 g, 1.50 mmol) and 1,10-phenanthroline (0.20 g, 1.00 mmol), both dissolved in absolute ethanol, were mixed (total volume ≈ 75 mL) and stirred for 15 min. The yellow solid formed was isolated by filtration and dried in air. Yield: 0.59 g (81%). $\text{C}_{66}\text{H}_{40}\text{Cl}_6\text{Mn}_3\text{N}_4\text{O}_{12}$ (1458.57 g mol^{-1}): calcd. C 54.35, H 2.76, Cl 14.58, N 3.84; found C 54.3, H 2.7, Cl 14.7, N 3.8. Yellow needlelike crystals, suitable for X-ray diffraction, were obtained by dissolving $[\text{Mn}(2\text{-ClC}_6\text{H}_4\text{COO})_2] \cdot n\text{H}_2\text{O}$ in CH_3CN and layering with 1,10-phenanthroline in CH_2Cl_2 in a 1:1 ratio. Selected IR data (KBr pellet): $\tilde{\nu} = 1607$ (vs), 1549 (m), 1514 (w), 1436 (w), 1420 (m), 1406 (s), 1387 (vs), 1051 (m), 862 (w), 843 (m), 762 (s), 727 (m), 648 (w), 464 (w) cm^{-1} .

$[\text{Mn}_3(\mu\text{-}3\text{-ClC}_6\text{H}_4\text{COO})_6(\text{phen})_2]$ (2): The same procedure was followed as for compound **1**, in this case with $[\text{Mn}(3\text{-ClC}_6\text{H}_4\text{COO})_2] \cdot n\text{H}_2\text{O}$. A yellow solid was formed, filtered and dried in air. Yield: 0.66 g (89%). $\text{C}_{66}\text{H}_{40}\text{Cl}_6\text{Mn}_3\text{N}_4\text{O}_{12} \cdot 0.5\text{H}_2\text{O}$ (1467.58 g mol^{-1}): calcd. C 54.01, H 2.82, Cl 14.49, N 3.82; found C 54.1, H 2.9, Cl 14.4, N 3.7. Selected IR data (KBr pellet): $\tilde{\nu} = 1606$ (vs), 1560 (vs), 1539 (m), 1516 (m), 1422 (m), 1392 (s), 867 (w), 846 (w), 763 (m), 748 (w), 731 (m), 675 (w), 657 (w), 639 (w), 439 (w) cm^{-1} .

$[\text{Mn}_3(\mu\text{-}4\text{-ClC}_6\text{H}_4\text{COO})_6(\text{phen})_2]$ (3): The same procedure for the preparation and crystallization of **1** was followed, by using $[\text{Mn}(4\text{-ClC}_6\text{H}_4\text{COO})_2] \cdot n\text{H}_2\text{O}$ instead. A yellow solid was formed, isolated by filtration and dried in air. Yield: 0.55 g (75%). $\text{C}_{66}\text{H}_{40}\text{Cl}_6\text{Mn}_3\text{N}_4\text{O}_{12} \cdot \text{H}_2\text{O}$ (1476.59 g mol^{-1}): calcd. C 53.68, H 2.87, Cl 14.41, N 3.79; found C 53.5, H 2.8, Cl 14.4, N 3.8. Yellow needlelike crystals, suitable for X-ray diffraction, were obtained when a solution of $[\text{Mn}(4\text{-ClC}_6\text{H}_4\text{COO})_2] \cdot n\text{H}_2\text{O}$ in $\text{CH}_3\text{CH}_2\text{OH}$ was layered with 1,10-phenanthroline dissolved in CH_2Cl_2 in a 1:1 ratio. Selected IR data (KBr pellet): $\tilde{\nu} = 1604$ (vs), 1557 (vs), 1538 (s), 1516 (m), 1406 (vs), 1091 (m), 1013 (m), 854 (m), 843 (m), 774 (s), 729 (m), 687 (w), 534 (m) cm^{-1} .

$[\text{Mn}(\mu\text{-}3\text{-ClC}_6\text{H}_4\text{COO})_2(\text{phen})]_n$ (4): 1,10-phenanthroline (0.30 g, 1.50 mmol) in absolute ethanol was added to a solution of $[\text{Mn}(3\text{-ClC}_6\text{H}_4\text{COO})_2] \cdot n\text{H}_2\text{O}$ (0.60 g, 1.50 mmol) in the same solvent. The resulting mixture (≈ 100 mL) was stirred for 15 min to give a pale yellow solid that was filtered and dried in air. Yellow crystals suitable for X-ray diffraction were obtained after several days by slow evaporation of the mother liquor in the refrigerator. Yield: 0.61 g (74%). $\text{C}_{26}\text{H}_{16}\text{Cl}_2\text{MnN}_2\text{O}_4$ (546.26 g mol^{-1}): calcd. C 57.17, H 2.95, Cl 12.98, N 5.13; found C 57.0, H 2.9, Cl 13.2, N 5.1. Selected IR data (KBr pellet): $\tilde{\nu} = 1653$ (vs), 1606 (s), 1562 (s), 1512 (w), 1422 (m), 1386 (vs), 1143 (w), 1068 (w), 862 (w), 849 (m), 761 (s), 730 (s) cm^{-1} .

$[\{\text{Mn}(4\text{-ClC}_6\text{H}_4\text{COO})(\text{phen})\}_2(\mu\text{-}4\text{-ClC}_6\text{H}_4\text{COO})_2(\mu\text{-H}_2\text{O})]$ (5): 1,10-phenanthroline (0.12 g, 0.63 mmol) in acetonitrile was added to a suspension of $[\text{Mn}(4\text{-ClC}_6\text{H}_4\text{COO})_2] \cdot n\text{H}_2\text{O}$ (0.25 g, 0.63 mmol) in the same solvent. The resultant mixture (total volume ≈ 50 mL) was stirred for about 15 min, and a yellow solid formed that was filtered and dried in air. Yellow crystals suitable for X-ray diffraction were obtained by slow evaporation of the mother liquor in the refrigerator after several days. Yield: 0.66 g (89%). $\text{C}_{52}\text{H}_{34}\text{Cl}_4\text{Mn}_2\text{N}_4\text{O}_9$ (1110.53 g mol^{-1}): calcd. C 56.24, H 3.09, Cl 12.77, N 5.05; found C 56.3, H 3.0, Cl 13.1, N 5.1. Selected IR data (KBr pellet): $\tilde{\nu} = 1606$ (vs), 1591 (s), 1556 (s), 1515 (m), 1423

Table 8. Crystallographic data for compounds **1**, **3**·2CH₂Cl₂, **4** and **5**.

	1	3 ·2CH ₂ Cl ₂	4	5
Chemical formula	$\text{C}_{66}\text{H}_{40}\text{Cl}_6\text{Mn}_3\text{N}_4\text{O}_{12}$	$\text{C}_{68}\text{H}_{44}\text{Cl}_{10}\text{Mn}_3\text{N}_4\text{O}_{12}$	$\text{C}_{26}\text{H}_{16}\text{Cl}_2\text{MnN}_2\text{O}_4$	$\text{C}_{52}\text{H}_{34}\text{Cl}_4\text{Mn}_2\text{N}_4\text{O}_9$
Formula weight	1458.54	1628.39	546.25	1110.51
Crystal colour, habit	yellow, prism	colourless, prism	needle, yellow	yellow, prism
T / K	100(2)	100(2)	100(2)	100(2)
$\lambda (\text{Mo-K}\alpha) / \text{\AA}$	0.7107	0.7107	0.7107	0.7107
Crystal system	triclinic	triclinic	monoclinic	monoclinic
Space group	$P\bar{1}$	$P\bar{1}$	$C2/c$	$I2/a$
Crystal size / mm	$0.24 \times 0.06 \times 0.04$	$0.15 \times 0.09 \times 0.07$	$0.25 \times 0.05 \times 0.02$	$0.21 \times 0.08 \times 0.07$
$a / \text{\AA}$	11.2545(3)	11.1636(4)	26.6151(11)	15.4589(17)
$b / \text{\AA}$	11.3480(3)	13.0051(5)	11.8583(5)	15.610(2)
$c / \text{\AA}$	13.1717(4)	13.2017(5)	7.2206(3)	20.154(3)
$\alpha / ^\circ$	68.8470(10)	72.328(2)	90	90
$\beta / ^\circ$	72.5150(10)	66.058(2)	94.008(3)	101.578(5)
$\gamma / ^\circ$	75.8420(10)	89.276(2)	90	90
$V / \text{\AA}^3$	1478.76(7)	1655.59	2273.32(16)	4764.4(12)
Z	1	1	4	4
$\rho_{\text{calcd.}} / \text{g cm}^{-3}$	1.638	1.633	1.596	1.545
μ / mm^{-1}	0.97	1.034	0.854	0.818
$F(000)$	737	821	1108	2256
θ range / $^\circ$	1.7–26.4	1.66–26.41	1.53–26.42	1.66–26.38
Index ranges	$-13 \leq h \leq 14$ $-12 \leq k \leq 14$ $0 \leq l \leq 16$	$-12 \leq h \leq 13$ $-15 \leq k \leq 16$ $0 \leq l \leq 16$	$-33 \leq h \leq 33$ $0 \leq k \leq 14$ $0 \leq l \leq 9$	$-19 \leq h \leq 18$ $0 \leq k \leq 19$ $0 \leq l \leq 25$
Data/restraints/parameters	6059/0/412	6797/9/449	4144/0/160	4881/0/325
Goodness-of-fit on F^2	0.991	1.043	0.920	1.055
$R_1^{[a]}, wR_2^{[b]}$ [$I > 2\sigma(I)$]	0.0377, 0.0754	0.0457, 0.1077	0.0457, 0.0867	0.0360, 0.0823
$R_1^{[a]}, wR_2^{[b]}$ (all data)	0.062, 0.0836	0.0562, 0.1147	0.1011, 0.0978	0.0481, 0.0869

[a] $R_1 = \sum |F_o| - |F_c| / \sum |F_o|$. [b] $wR_2 = \{\sum [w(F_o^2 - F_c^2)^2] / \sum [w(F_o^2)^2]\}^{1/2}$, $w = 1 / [\sigma^2(F_o^2) + (aP)^2 + bP]$, where $P = [\max(F_o^2, 0) + 2F_c^2] / 3$.

(s), 1399 (vs), 1089 (m), 1012 (m), 861 (m), 844 (s), 815 (m), 775 (s), 728 (m), 686 (w), 637 (w), 533 (s) cm⁻¹.

X-ray Structural Determination: Crystals of **1**, **3**, **4** and **5**, obtained as described in the experimental section, were mounted in air, and X-ray crystallographic data were collected at 100 K. All measurements were made on a Bruker Apex-II CCD diffractometer with graphite monochromated Mo-*K*_α radiation ($\lambda = 0.7107 \text{ \AA}$). The structures were solved by using the SIR97 program^[53] and refined with the SHELXL97 program.^[54] Hydrogen atoms were treated by a mixture of independent and constrained refinements. Crystal data collection and refinement parameters are given in Table 8.

CCDC-735801 (**1**), -735803 (**3**), -735802 (**4**) and -735804 (**5**) contain the supplementary crystallographic data for this paper. These data can be obtained free of charge from The Cambridge Crystallographic Data Centre via www.ccdc.cam.ac.uk/datarequest/cif.

Supporting Information (see footnote on the first page of this article): Variable-temperature X-band EPR spectra of the powdered sample of the 1D compound **4** (Figure S1). Variable-temperature X-band EPR spectra of the powdered sample of the neutral dinuclear compound **5** (Figure S2).

Acknowledgments

This work was supported by the Ministerio de Ciencia y Tecnología of Spain through the project CTQ2006-01759/BQU and the Comissió Interdepartamental de Recerca i Innovació Tecnològica of la Generalitat de Catalunya (CIRIT) (2005-SGR00593). V. G. thanks the Ministerio de Ciencia e Innovación for the PhD grant BES-2007-15668 and Gavin Craig for his help with English.

- [1] V. L. Pecoraro, *Manganese Redox Enzymes*, VHC Publishers, 1992.
- [2] M. Murrie, D. J. Price, *Annu. Rep. Prog. Chem. Sect. A* **2007**, 103, 20–38, and references cited therein.
- [3] A. J. Wu, J. E. Penner-Hahn, V. L. Pecoraro, *Chem. Rev.* **2004**, 104, 903–938.
- [4] C. S. Mullins, V. L. Pecoraro, *Coord. Chem. Rev.* **2008**, 252, 416–443.
- [5] S. L. Castro, Z. Sun, C. M. Grant, J. C. Bollinger, D. N. Hendrickson, G. Christou, *J. Am. Chem. Soc.* **1998**, 120, 2365–2375.
- [6] M. Kloskowski, D. Pursche, R.-D. Hoffmann, R. Pottgen, M. Lage, A. Hammerschmidt, T. Glaser, B. Krebs, *Z. Anorg. Allg. Chem.* **2007**, 633, 106–112.
- [7] Y. Chen, X.-W. Wang, B. Hu, F.-P. Chen, J.-Z. Chen, L. Chen, *J. Coord. Chem.* **2007**, 60, 2401–2408.
- [8] B.-H. Ye, X.-M. Chen, F. Xue, L.-N. Ji, T. C. W. Mak, *Inorg. Chim. Acta* **2000**, 299, 1–8.
- [9] H.-C. Yao, N. Wang, L. Zhang, Z.-J. Li, *Acta Crystallogr., Sect. E: Struct. Rep. Online* **2008**, 64, m774.
- [10] B. Kang, M. Kim, J. Lee, Y. Do, S. Chang, *J. Org. Chem.* **2006**, 71, 6721–6727.
- [11] C.-J. Shen, J.-S. Chen, T.-L. Sheng, R.-B. Fu, S.-M. Hu, S.-C. Xiang, Z.-T. Qin, X. Wang, Y.-M. He, X.-T. Wu, *Jiegou Huaxue (Chin. J. Struct. Chem.)* **2008**, 27, 899.
- [12] C. E. Anson, R. Langer, L. Ponikiewski, A. Rothenberger, *Inorg. Chim. Acta* **2005**, 358, 3967–3973.
- [13] S. G. Baca, Y. Sevryugina, R. Clerac, I. Malaestean, N. Gerbeleu, M. A. Petrukhina, *Inorg. Chem. Commun.* **2005**, 8, 474–478.
- [14] C. J. Milios, T. C. Stamatatos, P. Kyritsis, A. Terzis, C. P. Raptopoulou, R. Vicente, A. Escuer, S. P. Perlepes, *Eur. J. Inorg. Chem.* **2004**, 2885–2901.
- [15] Z. Chen, Y. Ma, F. Liang, Z. Zhou, *J. Organomet. Chem.* **2008**, 693, 646–654.
- [16] R. L. Rardin, P. Poganiuch, A. Bino, D. P. Goldberg, W. B. Tolman, S. Liu, S. J. Lippard, *J. Am. Chem. Soc.* **1992**, 114, 5240–5249.
- [17] S. G. Baca, I. L. Malaestean, T. D. Keene, H. Adams, M. D. Ward, J. Hauser, A. Neels, S. Decurtins, *Inorg. Chem.* **2008**, 47, 11108–11119.
- [18] A. Escuer, B. Cordero, X. Solans, M. Font-Bardia, T. Calvet, *Eur. J. Inorg. Chem.* **2008**, 5082–5087.
- [19] S. Menage, S. E. Vitols, P. Bergerat, E. Codjovi, O. Kahn, J.-J. Girerd, M. Guillot, X. Solans, T. Calvet, *Inorg. Chem.* **1991**, 30, 2666–2671.
- [20] V. Tangoulis, D. A. Malamataris, K. Soulti, V. Stergiou, C. P. Raptopoulou, A. Terzis, A. Kabanos, D. P. Kessissoglou, *Inorg. Chem.* **1996**, 35, 4974–4983.
- [21] B. Albela, M. Corbella, J. Ribas, I. Castro, J. Sletten, H. Stoeckli-Evans, *Inorg. Chem.* **1998**, 37, 788–798.
- [22] G. Fernandez, M. Corbella, J. Mahia, M. A. Maestro, *Eur. J. Inorg. Chem.* **2002**, 2502–2510.
- [23] C. C. Stoumpos, I. A. Gass, C. J. Milios, E. Kefalloniti, C. P. Raptopoulou, A. Terzis, N. Lalioti, E. K. Brechin, S. P. Perlepes, *Inorg. Chem. Commun.* **2008**, 11, 196–202.
- [24] H. Hou, L. Li, Y. Zhu, Y. Fan, Y. Qiao, *Inorg. Chem.* **2004**, 43, 4767–4774.
- [25] M. Andruh, H. W. Roesky, M. Noltemeyer, H.-G. Schmidt, *Polyhedron* **1993**, 12, 2901–2903.
- [26] C.-G. Zhang, J. Sun, X.-F. Kong, C.-X. Zhao, *J. Chem. Crystallogr.* **1999**, 29, 199–201.
- [27] J. Li, J. Zhang, A. Wu, Y. Xi, H. Guo, F. Zhang, *Sci. China, Ser. B: Chem.* **2005**, 48, 79–82.
- [28] C.-S. Liu, J.-R. Li, C.-Y. Li, J.-J. Wang, X.-H. Bu, *Inorg. Chim. Acta* **2007**, 360, 2532–2540.
- [29] H.-X. Guo, J.-X. Chen, Q.-H. Wang, X.-L. You, *Acta Crystallogr., Sect. E: Struct. Rep. Online* **2007**, 63, m915–m917.
- [30] M. Devereux, M. Curran, M. McCann, M. T. Casey, V. McKee, *Polyhedron* **1996**, 15, 2029–2033.
- [31] J. Wang, M.-H. Huang, P. Liu, W.-D. Cheng, L.-M. Zhang, *Jiegou Huaxue (Chin. J. Struct. Chem.)* **2007**, 26, 139.
- [32] C.-H. Zhang, C.-H. Li, D.-Z. Kuang, M.-S. Chen, W. Li, Y.-Q. Yang, Y.-F. Kuang, *Wuji Huaxue Xuebao (Chin. J. Inorg. Chem.)* **2007**, 23, 1255.
- [33] J.-R. Su, D.-J. Xu, *Acta Crystallogr., Sect. C: Cryst. Struct. Commun.* **2005**, 61, m256–m258.
- [34] A. Karmakar, K. Bania, A. M. Baruah, J. B. Baruah, *Inorg. Chem. Commun.* **2007**, 10, 959–964.
- [35] B.-H. Ye, I. D. Williams, X.-Y. Li, *J. Inorg. Biochem.* **2002**, 92, 128–136.
- [36] S. G. Shova, L. G. Turyatke, G. V. Novitsky, M. D. Mazus, A. P. Gulya, *Koord. Khim.* **1996**, 22, 517.
- [37] Y.-Q. Yang, C.-H. Li, W. Li, Y.-F. Kuang, *Jiegou Huaxue (Chin. J. Struct. Chem.)* **2008**, 27, 149.
- [38] Y.-L. Shen, S.-L. Sun, W.-D. Song, *Acta Crystallogr., Sect. E: Struct. Rep. Online* **2007**, 63, m1309–m1311.
- [39] W. Li, C.-H. Li, Y.-Q. Yang, Y.-F. Kuang, *Jiegou Huaxue (Chin. J. Struct. Chem.)* **2007**, 26, 1057.
- [40] R. A. Reynolds III, W. R. Dunham, D. C. Coucouvanis, *Inorg. Chem.* **1998**, 37, 1232–1241.
- [41] A. Caneschi, F. Ferraro, D. Gatteschi, M. C. Melandri, P. Rey, R. Sessoli, *Angew. Chem. Int. Ed. Engl.* **1989**, 28, 1365–1367.
- [42] S.-B. Yu, S. J. Lippard, I. Shweky, A. Bino, *Inorg. Chem.* **1992**, 31, 3502–3504.
- [43] B.-H. Ye, T. Mak, I. D. Williams, X.-Y. Li, *Chem. Commun.* **1997**, 1, 813–1814.
- [44] D. Coucouvanis, R. A. Reynolds III, W. R. Dunham, *J. Am. Chem. Soc.* **1995**, 117, 7570–7570.
- [45] R. L. Rardin, W. B. Tolman, S. J. Lippard, *New J. Chem.* **1991**, 15, 417–430.
- [46] K. Kambe, *J. Phys. Soc. Jpn.* **1950**, 5, 48–51.
- [47] J. H. Van Vleck, *The Theory of Electric and Magnetic Susceptibilities*, Oxford University Press, London, 1932.
- [48] O. Kahn, *Molecular Magnetism*, Wiley-VCH Inc., 1993.

- [49] M. E. Fisher, *Am. J. Phys. Rev. A* **1964**, 32, 343–346.
- [50] S. Durot, C. Policar, G. Pelosi, F. Bisceglie, T. Mallah, J. P. Mahy, *Inorg. Chem.* **2003**, 42, 8072–8080, and references cited therein.
- [51] S. Stoll, A. Schweiger, *J. Magn. Reson.* **2006**, 178, 42–55.
- [52] A. Bencini, D. Gatteschi, *Electron Paramagnetic Resonance of Exchange Coupled Systems*, Springer-Verlag, Berlin, Heidelberg, **1990**.
- [53] *SIR97: A New Tool for Crystal Structure Determination and Refinement*, A. Altomare, M. C. Burla, M. Camalli, G. L. Cascarano, C. Giacovazzo, A. Guagliardi, A. G. G. Moliterni, G. Polidori, R. Spagna, *J. Appl. Crystallogr.* **1999**, 32, 115–119.
- [54] G. M. Sheldrick, *SHELXL97: A Program for Crystal Structure Refinement*, University of Göttingen, Germany, **1997**.

Received: June 14, 2009

Published Online: September 2, 2009